Nanoscale

PAPER

View Article Online
View Journal | View Issue

Cite this: *Nanoscale*, 2026, **18**, 5436

Controlled synthesis of copper oxide nanoparticles (CuONPs) by the precipitation method and proposition of their growth mechanism

Fadoua Sallem, *[a] Corinne chanéac, [b] Mickael Wagner, [a] Nicolas Rataj,[a] Eloise Annabi,[a] Alain Castillo,[a] Ludovic Menjot[a] and Astrid Avellan [a]

Received 14th November 2025,
Accepted 14th January 2026

DOI: 10.1039/d5nr04826e

rsc.li/nanoscale

This study presents an investigation into the surfactant-free synthesis of copper oxide nanoparticles (CuONPs) *via* a precipitation method, focusing on how various experimental parameters influence nanoparticle characteristics. By varying key parameters, such as precursor type and concentration, pH, and reaction temperature, the work reveals their impact on nanoparticle size, morphology, and crystallinity. The results highlight that the precursor's counter-ion and Cu/OH ratio play key roles in directing the particle shape, while an increased copper concentration favored rod-like structures through an oriented attachment phenomenon. A temperature-dependent phase transition was observed for the first time, illustrating a metastable flake-like intermediate that transforms into spherical nanoparticles at high temperatures. This study proposes a detailed growth mechanism, identifying two temperature-dependent pathways, slow CuO condensation at low temperatures and competing oxolation/olation reactions at high temperatures. Overall, this work establishes a reproducible framework for tailoring the morphology of CuONPs under mild conditions.

Introduction

Copper oxide (CuO) is a transition metal oxide that exhibits interesting physical–chemical properties, including a narrow bandgap of 1.2 eV, superthermal conductivity, high stability, and antimicrobial activity.[1] Copper oxide nanoparticles (CuONPs) with their small size and large surface area have attracted attention and find widespread use in electronic,[2] health,[3,4] water treatment,[5] textiles,[6] environment,[7] and food and agricultural processing applications.[8,9] Good control over the synthesis of CuONPs is needed to tune their properties and applications.

Various strategies and methods for synthesizing CuO nanostructures have been studied, each offering distinct control over the morphology, size, and properties of the resulting material. Common synthesis techniques include hydrothermal, sol–gel, electrochemical deposition, sonochemical, precipitation, and microwave methods.[10] Hydrothermal methods allow for precise control over particle size and shape by varying the temperature, precursor concentration, and reaction time, leading to CuO nanostructures ranging from nanoneedles to nanosheets and nanowires.[11–13] Sol–gel processes, on the other hand, utilize organic and inorganic precursors to form CuO with tailored surface characteristics. However, a calcination step is required to remove the organic matter and enhance the crystallinity of the materials.[14] The precipitation approach, or "direct solution method", is simple and more cost-efficient than the other synthesis protocols. It is based on the precipitation of ionic copper into copper hydroxide and then its condensation into copper oxide when it is mixed with an alkaline hydroxide according to following equations:

$$[Cu(OH_2)_6]^{2+} + 2OH^- \rightarrow [Cu(OH)_2(OH_2)_4]^0 + 2H_2O \quad (1)$$

$$[Cu(OH)_2(OH_2)_4]^0 \rightarrow Cu(OH)_2(s) + 4H_2O \quad (2)$$

$$Cu(OH)_2(s) \rightarrow CuO(s) + H_2O \quad (3)$$

The precipitation method is very simple to perform, does not require harmful solvents or reagents, and can be carried out under mild reaction conditions in a short period of time. However, the synthesis of nanosized copper oxide particles remains a challenging task where the growth mechanism is still not well discussed in the literature. Indeed, the most common CuO nanostructure morphologies, whose growth mechanisms have been discussed in the literature, with different synthesis methods, are flakes or a petal-shaped form,[15] flower-shaped particles,[16] and nanoneedles.[17] However, there is no study that discusses the synthesis mecha-

[a]*Géosciences-Environnement-Toulouse (GET), UMR 5563 CNRS, UPS, IRD, CNES, OMP, 14, Avenue Edouard Belin, F-31400 Toulouse, France.*
E-mail: fadouasallem@gmail.com
[b]*Laboratoire de Chimie de la Matière Condensée de Paris (LCMCP), CNRS, Sorbonne Université, Paris, 75005 France*

nism of spherical shaped nanoparticles. Moreover, controlling the growth mechanism of CuONPs using the precipitation method without the use of surfactants is still not well understood, despite the effort of some studies to understand the role of some experimental parameters.[18–20]

There is no universal growth mechanism that can explain the formation of all CuONP sizes and morphologies, as the process is strongly influenced by the specific experimental conditions. Although the general steps of nanoparticle synthesis through the precipitation method are well established, the precise influence of each experimental parameter on the reaction steps—and consequently on the physicochemical properties of the resulting particles—remains poorly understood. In solution, copper ions exist as hexahydrated complexes ($[Cu(H_2O)^6]^{2+}$) that undergo hydroxylation after adding an alkaline hydroxide (reaction (1)). The resulting hydroxylated complexes ($[Cu(OH)_2(H_2O)_4]^0$) are unstable and condense *via* two successive reactions: olation, involving water elimination to form hydroxo bridges and precipitation of crystallized ($Cu(OH)_2$) nanoparticles (reaction (2)), and then oxolation, which produces oxo bridges *in situ*, with water elimination leading to the formation of the oxide phase (CuO) (reaction (3)).[21] Therefore, understanding how experimental parameters influence each step of the growth mechanism is essential to control the size and shape of the resulting nanoparticles.

Experimental parameters in the precipitation method such as the type and concentration of the precursor, pH, reaction temperature, the choice of the surfactant and the solvent used play critical roles in determining the crystalline phase, size and morphology of CuONPs.[1] The pH of the solution, for example, can significantly influence the morphology of CuO, with acidic conditions favoring the formation of nanorods and alkaline conditions promoting nanosheet growth.[22] One of the most influential parameters affecting the morphology and crystallinity of CuONPs is the reaction temperature.[19] While the impact of temperature has been extensively investigated in the literature for different methods of CuONP synthesis, especially the hydrothermal synthesis,[23] only a few studies have examined its effect in the precipitation method where its role remains insufficiently discussed.

The effect of the starting materials has not been extensively discussed in the literature because it was considered that any kind of soluble copper salts and alkali hydroxide compounds could be used for the synthesis of CuONPs.[1] According to the literature, copper acetate and copper nitrate are the most commonly used copper precursors, while sodium hydroxide is the most frequently employed hydroxide source.[19,24,25]

H. Siddiqui *et al.*[18] investigated the effect of copper salts by comparing copper nitrate and copper chloride as precursors. They showed distinct nanoparticle morphologies depending on the copper precursor used. However, their synthesis protocol included the surfactant hexamethylenetetramine (HMT), which may interact with sodium hydroxide and alter the growth mechanism. Similarly, the concentration of the reagent is another parameter often overlooked in the literature,[26] despite being a well-known key factor influencing the growth rates of materials.[27] Indeed, low precursor concentrations typically result in smaller particles with a narrow size distribution.[1]

In this work, we aim to extensively investigate the effect of all the key experimental parameters that control the synthesis of CuONPs, such as the precursors (type and concentration), the reaction temperature and pH. This study also aims to understand how these parameters influence the morphology and the final physicochemical properties of the nanoparticles. It suggests a growth mechanism for the precipitation synthesis of copper-based nanoparticles without the use of any surfactant by investigating the intermediate synthesis steps. Indeed, understanding these effects is crucial for establishing the relationship between the experimental conditions and the properties of the resulting CuONPs. This also contributes to more precise and reproducible synthetic strategies for tailoring nanomaterials for specific applications. To do so, transmission electron microscopy (TEM) was used for a detailed morphological study and X-ray diffraction (XRD) and specific surface area analyses were performed for structural study.

Materials and methods

Reagents

Copper nitrate trihydrate ($Cu(NO_3)_2{\cdot}3H_2O$, >99%), copper sulfate anhydrous ($CuSO_4$, >98%), potassium hydroxide (KOH, >85%), copper acetate monohydrate ($Cu(CH_3COO)_2{\cdot}H_2O$, >98%) and sodium hydroxide (NaOH, 98.5%) were purchased from Fisher Scientific. Ammonium hydroxide solution (NH_4OH, 28–30%) was purchased from Merck. Deionized (DI) water was produced using a Milli-Q EQ 7008 system from Merck. All chemicals were used as received without any purification.

Synthesis of CuONPs using the precipitation method

Various synthesis parameters were tested (Fig. 1). A specific concentration of blue-colored copper solution ($Cu(NO_3)_2{\cdot}3H_2O$, $CuSO_4$ or $Cu(CH_3COO)_2{\cdot}H_2O$ (0.02, 0.04, 0.06, 0.1, 0.2, 0.5 M)) was prepared in 150 mL of deionized (DI) water in a 250 mL three neck flask. The solution was heated at different temperatures (T = 25, 50, 60, 70, 80, and 95 °C) under vigorous magnetic stirring for 10 minutes and then a specific amount of hydroxide reagent (NaOH, KOH, NH_4OH) was added into the solution to obtain a Cu : OH 1 : 2 molar ratio, the stoichiometry required to generate the neutral precursor (reaction (1)). Two additional Cu : OH molar ratios (1 : 4 and 1 : 6) were also studied for NaOH. Additional experiments were performed for T = 25, 60 and 70 °C, where the mixture was heated at boiling temperature for 15 min immediately upon addition of the base. At the end of the reaction, all samples were cooled down very fast using an ice bath in order to avoid any morphological evolution due to the temperature during the cooling process. The obtained suspension was washed twice with deionized (DI) water using centrifugation and finally freeze-dried for at least 48 h.

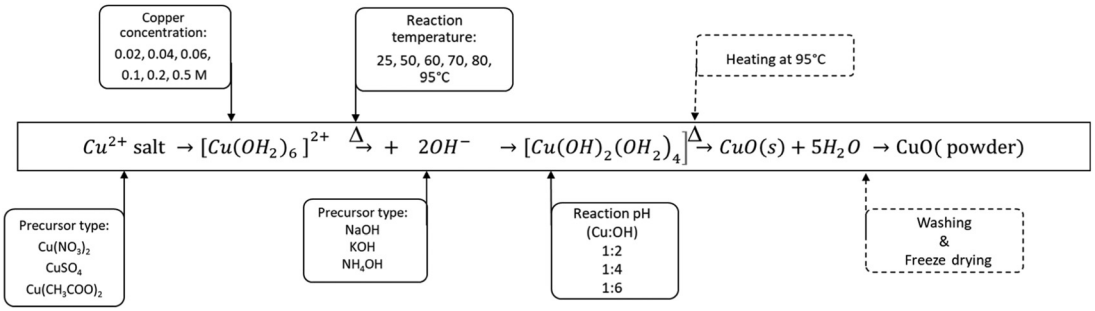

Fig. 1 Illustration of the precipitation reaction of Cu^{2+} ions and the studied experimental parameters.

Characterization techniques

Transmission Electron Microscopy (TEM) characterization studies were performed using a JEOL JEM 1011 microscope operating at 100 kV (point-to-point resolution of 0.45 nm). High-resolution transmission electron microscopy (HRTEM) was also used to obtain high-resolution TEM images using a JEOL JEM 2100F microscope operating at 200 kV (point-to-point resolution of 0.19 nm).

The samples were prepared by evaporating a drop of a diluted suspension of CuONPs in DI water on a carbon-coated nickel grid. About one hundred nanoparticles were counted for statistical size calculation using ImageJ software.

X-ray powder diffraction patterns were recorded using a D8 Advanced Bruker diffractometer with CuK_α radiation (λ = 1.54060 Å) over the 2θ range of 2–80° in steps of 0.0098° per 0.4 s. The data analysis was carried out using Diffrac.EVA software.

Specific surface area measurements (S_{BET}) were carried out using a Quantachrome Autosorb iQ instrument. Samples were outgassed at 100 °C for 14 h. The measurements were performed at liquid nitrogen temperature using N_2 as the adsorbing gas. The BET method was used in the calculation of the surface area value from the isotherm of nitrogen adsorption.

Zeta potential measurements were carried out using an Amerigo Zetasizer (Cordouan Technologies). All samples were analyzed after the washing step in a suspension form at a concentration of about 50 μg mL^{-1}.

Results and discussion

Effect of precursor type on the morphology of copper oxide nanoparticles (CuONPs)

To investigate the effect of the starting materials, three types of copper salts (nitrate, acetate, and sulfate) were tested with sodium hydroxide ([OH^-] = 0.04 M) and three types of hydroxide sources (ammonium, potassium and sodium) were tested with copper nitrate ([Cu^{2+}] = 0.02 M). The precipitation was performed at 95 °C for all experiments. The XRD patterns in Fig. 2 show that all samples crystallize in a monoclinic phase with the space group $C2/c$ of copper oxide in accordance with the black color of solids, with the following lattice parameters:

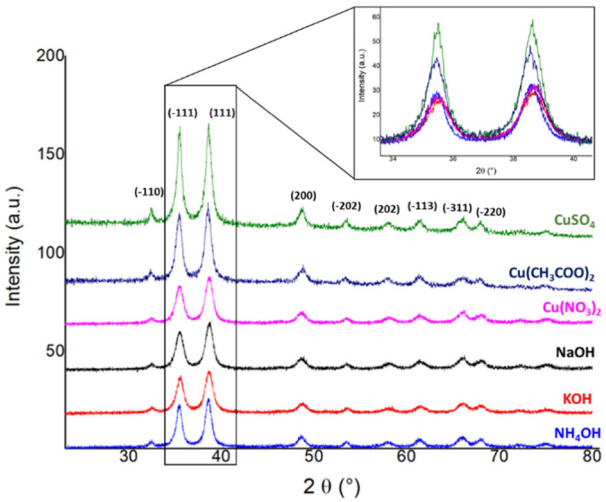

Fig. 2 XRD patterns of CuONPs synthesized with three different Cu precursors: nitrate, acetate and sulfate and OH sources: NaOH, KOH and NH_4OH at 95 °C ($\lambda K\alpha$ = 1.54060 Å).

a = 4.68530 Å, b = 3.42570 Å, and c = 5.13030 Å. The XRD peaks were indexed with powder diffraction file no. 00-045-0937 (tenorite). The intensity ratios of the (−111) and (111) peaks of all samples compared to those of the sample synthesized from copper nitrate and sodium hydroxide (taken as the reference) are shown in Table S1. It shows a high ratio for the CuONPs synthesized from acetate (2.4- and 2.8-fold) and sulfate copper salt (3.2- and 3.9-fold). However, a slight increase is found for the potassium and ammonium hydroxide precursors with intensity ratios 1.4- and 1.3-fold, and 1.7- and 1.6-fold higher, respectively. This result suggests higher crystallinity and preferential crystal growth of the copper sulfate and acetate-based samples compared to those obtained from copper nitrate salt (using NaOH as the hydroxide) and those obtained from KOH and NH_4OH (using copper nitrate as the salt). The average crystallite sizes were found to be 12.9 ± 3.3, 16.5 ± 5.4 and 19.1 ± 5.9 nm for the nitrate, acetate and sulfate precursors, respectively (using NaOH as the hydroxide), and 12.9 ± 3.3, 15.0 ± 5.7 and 17.1 ± 4.7 nm for NaOH, KOH and NH_4OH, respectively (using the copper nitrate form), according to the Debye–Scherrer equation[18] (Table S1). This indicates a slightly smaller

nanoparticle size for the nitrate-based CuONPs using NaOH as the hydroxide. Moreover, the narrow crystallite size distribution of this sample suggests an isotropic shape compared to all other samples where the crystallite size distribution is larger which suggests an anisotropic shape (Table S1). The largest crystallite size is observed for copper sulfate using NaOH as the hydroxide. However, there are comparable crystallite sizes for the remaining samples. The results indicate structural differences between the samples and imply morphological changes that the XRD data alone are insufficient to fully elucidate.

Fig. 3 shows the TEM images of CuONPs synthesized from three kinds of copper precursors (nitrate, acetate, and sulfate) using sodium hydroxide as the hydrolyzing agent and three kinds of hydroxide salts (sodium, potassium and ammonium) using copper nitrate as the copper salt. This figure indicates that only copper nitrate produced homogeneous quasi-spherical nanoparticles with a size of 11.8 ± 1.3 nm diameter since the use of acetate and sulfate salts leads to heterogeneously sized anisotropic particles, nanorods and nanoribbons with sizes of 18.6 ± 6.7 nm (8.8 ± 2.0 nm width) and 71.9 ± 55.1 nm (26.7 ± 9.9 nm width), respectively. Similar results were obtained for sodium hydroxide in comparison with potassium hydroxide and ammonia. Indeed, only NaOH leads to homogenously sized quasi-spherical nanoparticles (11.8 ± 1.3 nm), whereas KOH and NH_4OH form nanoribbons with sizes of 51.6 ± 33.6 nm (9.7 ± 4.3 nm width) and 34.6 ± 13.4 nm (9.7 ± 2.7 nm width), respectively. The TEM images reveal a significant change in the morphology of the samples depending on both the copper salt and the hydroxide source used. While the particles are quasi-spherical in the case of copper nitrate precipitation with NaOH, an increase in shape anisotropy is observed for copper acetate, leading to the formation of short nanorods (18.6 ± 6.7 nm length and 8.8 ± 2.0 nm width),

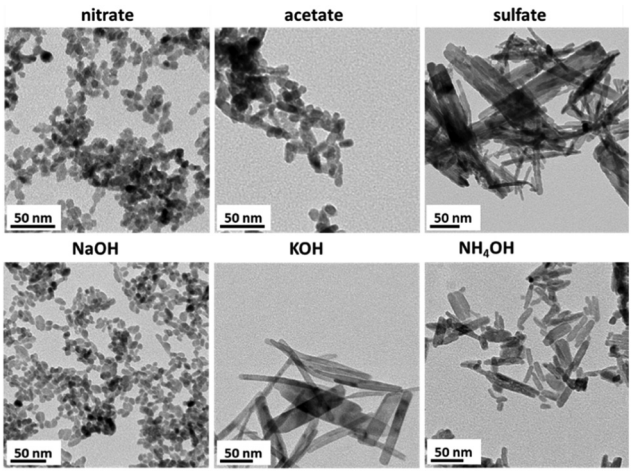

Fig. 3 TEM images of CuONPs obtained from different copper salts: nitrate, acetate and sulfate (using sodium hydroxide as the alkali hydroxide source) at 0.02 M and different hydroxide precursors: NaOH, KOH and NH_4OH (using copper nitrate as the copper salt) at 0.04 M (reaction temperature is 95 °C).

which is even more pronounced for copper sulfate that produces nanoribbons (71.9 ± 55.1 nm length and 26.7 ± 9.9 nm width). On the other hand, the zeta potential measurements of all samples, reported in Table S1, did not show significant differences between the samples because the counter ions were removed during the washing step. This does not allow one to conclude regarding the effect of the precursor on the surface charge of the obtained nanomaterials.

The obtained results demonstrate the importance of the choice of the starting materials for controlling the shape of CuONPs. A similar behavior was observed in the case of zinc oxide nanoparticles[28] and iron oxide nanoparticles.[29,30] Indeed, one possible explanation of the impact of the salt precursor is that the size and morphology of the nanoparticles are determined by a complex interplay between nucleation–growth kinetics, thermodynamic stability, and crystallographic constraints. Variations in the nucleation rates and growth dynamics influence whether particles develop isotropically or acquire anisotropic shapes. The crystallographic structure of the material is a critical factor, as different crystal facets possess distinct surface energies, which in turn govern preferential growth directions. These surface energies can also be substantially modified by the adsorption of ions or molecules onto the particle surface.[31–33] Such adsorption, originating from the synthesis medium or introduced deliberately through surfactants and capping agents, can selectively stabilize specific facets, thereby altering the particle's final morphology. Consequently, the competition between kinetic and thermodynamic factors, modulated by surface chemistry, dictates the ultimate size, shape, and structural characteristics of the nanoparticles. Subtle adjustments in synthesis conditions may therefore lead to pronounced variations in their physical properties.

Such shape anisotropy has already been reported for CuO syntheses using copper chloride and copper sulfate as precursors.[34] The present results suggest a relative complexing ability of the anions toward metal oxide surfaces, which follows the order $SO_4^{2-} > CH_3COO^- > NO_3^-$. This hierarchy reflects the differences in charge, polarizability, and coordination capability. The sulfate ion, being divalent and highly polarizable, can establish strong bidentate or bridging interactions with surface Cu^{2+} sites, stabilizing specific CuO facets. The acetate ion, with its carboxylate group, forms moderate monodentate or bidentate bonds, partially controlling crystal growth. In contrast, the nitrate ion interacts mainly through weak electrostatic attraction, exerting little influence on the morphology and stability of the CuO nanoparticles.

The same trend is observed for the cations originating from the base used during precipitation. While sodium showed no influence on the crystallographic orientation of the CuO particles, both ammonium (NH_4^+) and potassium (K^+) exhibited stronger interactions with the surface, promoting anisotropic particle growth. Although the ammonium ion itself possesses negligible complexing ability toward metal oxide surfaces and mainly interacts through weak electrostatic adsorption, its conjugate base, ammonia (NH_3), is a strong ligand capable of

coordinating to surface Cu^{2+} sites and thus affecting oxide formation mechanisms. The effect is even more surprising and unprecedented in the case of potassium, which is typically regarded as a non-complexing cation with no direct chemical interaction with oxide surfaces. Overall, the experimental results suggest the following order in their ability to enhance the anisotropy of CuO particles: $Na^+ < NH_4^+ < K^+$. This paragraph concludes that the choice of the starting material is crucial for controlling the shape of the final nanoparticles. In this section, five precursor combinations have been studied, namely $Cu(NO_3)_2$/NaOH, $Cu(NO_3)_2$/KOH, $Cu(NO_3)_2$/NH_4OH, $Cu(CH_3COO)_2$/NaOH and $CuSO_4$/NaOH, but there are so many other precursor combinations that were not studied and could lead to similar or different morphologies from those reported in this manuscript.

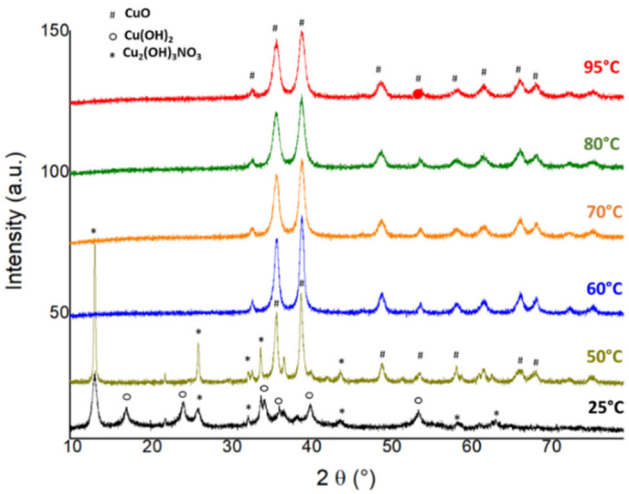

Fig. 4 XRD patterns of the copper-based structures obtained at different synthesis temperatures.

Temperature effect on crystal phases and their shape

To investigate the temperature effect, sodium hydroxide ($[OH^-]$ = 0.04 M) was added at different temperatures into an aqueous solution of copper nitrate at a concentration of 0.02 M. XRD analyses of the copper-based structures synthesized at different temperatures, presented in Fig. 4, showed a difference in the diffraction pattern between samples. Indeed, when adding NaOH at room temperature (25 °C), the color of the obtained powder is blue, which suggests the copper hydroxide phase. This was confirmed by the XRD results that showed a mixture of copper hydroxide ($Cu(OH)_2$), which crystallizes in the orthorhombic phase (JCPDS card no. 01-080-0656), and monoclinic copper hydroxynitrate ($Cu_2(OH)_3(NO_3)$) (JCPDS card no. 77-0148). For the sample synthesized at 50 °C, the color of the solid which was initially blue turned black at the end of the synthesis. The XRD pattern shows a mixture of two crystal phases of copper oxide (CuO) and copper hydroxynitrate. The hydroxynitrate phase is comprised of copper hydroxide layers in which some of the hydroxyl ions are replaced by nitrate ions and are directly coordinated to the sheets.[35] Above 50 °C (60–95 °C), there is only a copper oxide crystal phase where the color of the solid is black. The presence of a copper hydroxide crystal phase at a low synthesis temperature indicated that the oxolation step of the condensation mechanism of CuO did not occur at 25 °C and started at 50 °C, showing that copper oxide is the thermodynamically stable phase at these temperatures. Moreover, the modifications of the crystal phase with increasing temperature could also suggest morphological changes. On the other hand, the specific surface area measurements, shown in SI 1 (Fig. S1), show an increase as a function of the reaction temperature, which could also suggest a decrease in particles size and/or morphological changes, as discussed below.

Morphological analyses of the samples synthesized at different temperatures were performed, and the obtained TEM

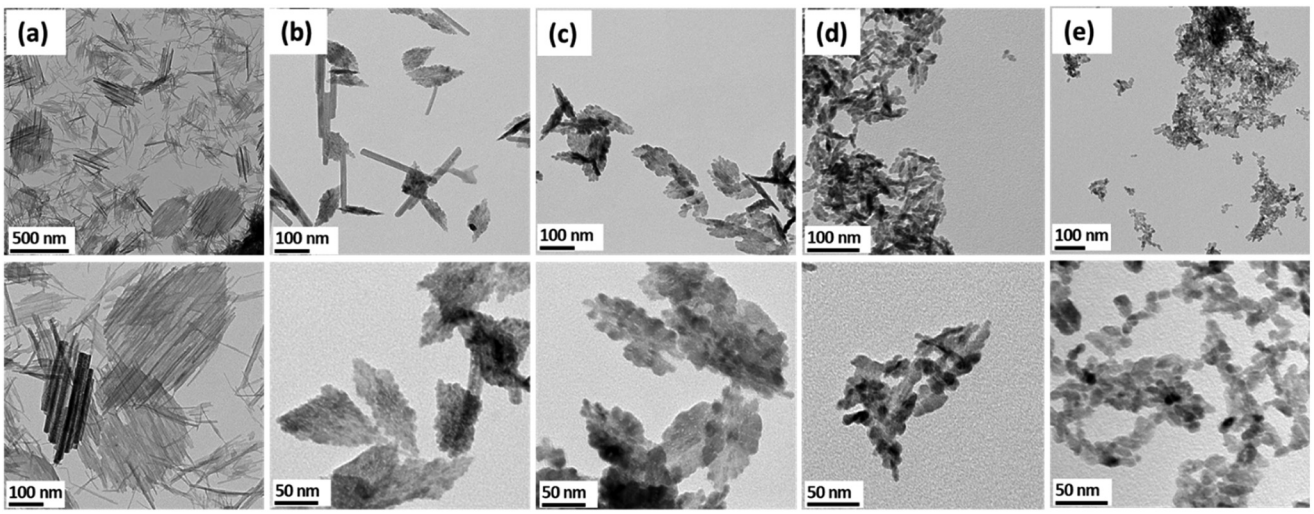

Fig. 5 TEM images of the copper (nano)-structures synthesized at different temperatures: (a) 25 °C, (b) 50 °C, (c) 60 °C, (d) 70 °C and (e) 90 °C using copper nitrate and sodium hydroxide ($[Cu^{2+}]$ = 0.02 M).

images are presented in Fig. 5. It shows temperature-dependent morphologies, as observed for the crystal phase change. Indeed, when NaOH was added at room temperature (25 °C), "lamella"-shaped morphologies were generated, which agglomerated according to the major axis to form "flake-shaped" structures according to an oriented attachment (OA) process.[19,36] However, at 50 °C, the same flake-shaped morphologies formed, but with an assembly of isotropic particles. The size of these structures at both temperatures was about 300 nm (Fig. 5a and b). When NaOH was added at a high temperature (between 60 and 90 °C), the submicron-sized structures started to disappear and nanosized particles formed instead. In fact, at 60 and 70 °C (Fig. 5c and d), the transition step from submicron to nano-sized particles is clearly visible where the flake-shaped structures begin to decompose into small nanoparticles. This result indicates that the temperature of NaOH addition is a crucial parameter that could drastically change the morphology of CuONPs.

The effect of temperature was also investigated by Zhu *et al.* who controlled the shape of CuONPs by changing the temperature of NaOH addition.[19] They obtained rod-shaped particles when NaOH was added at 100 and 60 °C and flake-shaped particles at 25 and 2 °C. However, this is the first time that the transition step is observed, illustrating the rearrangement phenomenon of CuO crystals to form nanoparticles from flake-shaped particles. One possible explanation of the temperature effect is that at 25 °C, there is a precipitation of the neutral precursor $[Cu(OH)_2(H_2O)_4]^0$ in the form of lamellar aquohydroxo complexes through olation reactions, which are the construction units of the flake-shaped particles, as shown in Fig. 6. At intermediate temperatures (50–70 °C), the hydroxide phase becomes unstable due to the spatial proximity of hydroxyl groups located between adjacent layers of the lamellar structure. This instability leads to oxolation reactions between the layers, driving the transformation of the hydroxide into the oxide. The increase in structural compactness during the oxolation reaction (increase in density from 3.37 g cm^{-3} for the hydroxide to 6.31 g cm^{-3} for the oxide) imposes significant internal constraints, which in turn result in fragmentation of the lamellar shapes into spherical particles. However, at high temperatures (above 80 °C), copper oxide particles are directly produced, as the oxolation reaction is thermally catalyzed (Fig. 6).

Growth mechanism

For a better understanding of the temperature effect and the growth mechanism of CuONPs, and the intermediate steps to form nanosized particles, NaOH was added at 25 °C, 60 °C and 70 °C (Fig. 5a, c and d, respectively) and then the solution was heated at the boiling point. The aim of this step is to understand the transition mechanism from submicron flake-shaped particles to quasi-spherical nanoparticles. The choice of temperature (60 and 70 °C) is based on the previous section results where the transition steps were mostly happening at these temperatures.

The morphologies of the obtained copper structure are presented in Fig. 7. Images a1 and a2 in Fig. 7 show that heating at 100 °C of the flake shaped-particles, initially synthesized at 25 °C and which are in the hydroxide form, kept the same shape but increased their size to 572 ± 153 nm and transformed them into more dense morphologies in the form of copper oxide (CuO) (XRD patterns in Fig. S2). This result is coherent with those obtained in the literature under the same experimental conditions.[19,37–39] One hypothesis of the obtained results is that at a low temperature, the reaction kinetics are low, so the olation step to form copper hydroxide takes time to occur. As the hydroxide is unstable under the heating conditions, it transforms into an oxide by the oxolation reaction between the slabs of the hydroxide lamellar structure, increasing the compactness of materials as it was mentioned in the previous section. This slower condensation reaction leads to the flake shape with a bigger size and explains the obtained morphology.

At higher temperatures (60 and 70 °C), there is a local rearrangement of the crystal plane, leading to more and more individualized and spherical-shaped nanoparticles with increasing temperature. Indeed, images b1,2 and c1,2 in Fig. 7 show

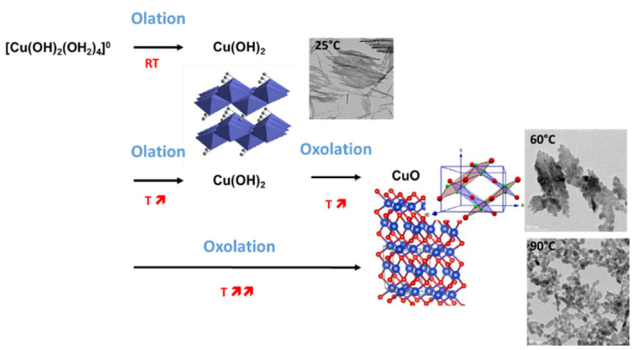

Fig. 6 Scheme illustrating the role of olation and oxolation reactions as a function of reaction temperature, along with the corresponding TEM images.

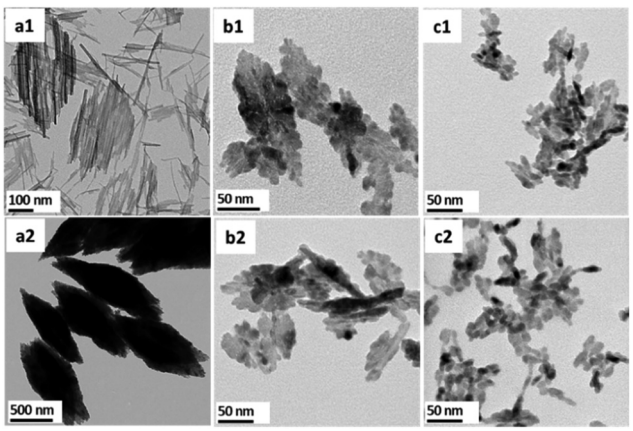

Fig. 7 TEM images of CuONPs synthesized at (a1) 25 °C, (b1) 60 °C and (c1) 70 °C and then heated at 100 °C to obtain (a2), (b2) and (c2), respectively.

further fragmentation of flake-shaped particles into more separated debris and fragments of nanoparticles. This phenomenon is illustrated by the high-resolution TEM (HRTEM) images of sample b2 in Fig. 7 shown in Fig. 8a and b, which suggest *in situ* rearrangement of flake-shaped CuO through a dissolution–crystallization phenomenon under the effect of the temperature. Additional HRTEM images are shown in Fig. S3. Indeed, at a high temperature, the reaction kinetics are high, resulting in a competition between the olation and oxolation mechanisms that occur at the same time, with the oxolation reaction being favored.[40] This leads to the production of nanoparticles inside the flake-shaped structures that are still attached with weaker bonds. These structures present some defects that facilitate the fragmentation of flake-shaped particles under the heating effect. In fact, heating at a higher temperature during the second step breaks these bonds and leads to more "free" nanoparticles.

This explains the difference between images b1,c1 and b2, c2. These results contradict the findings in the literature, which suggest that flake-shaped copper oxide is formed through the aggregation of $Cu(OH)_2$ nuclei.[16,41]

Precursor concentration effect

XRD analyses of the copper-based samples that were synthesized using different copper concentrations at 95 °C with the same Cu^{2+}/OH^- ratio (1 : 2) are presented in Fig. 9. It shows two crystal phases: one is copper oxide (CuO) for the samples that are synthesized at copper concentrations between 0.02 M and 0.1 M and the other is copper hydroxynitrate ($Cu_2(OH)_3(NO_3)$) for concentrations of 0.2 M and 0.5 M. The increase in the precursor concentration increased the growth rate of the nanoparticles. The presence of a copper hydroxynitrate phase at concentrations of 0.2 M and 0.5 M suggests that the oxolation step was not completed under these experiment conditions, which may be because of agglomeration of the nanoparticles that limited the access to hydroxyl groups at high ionic strengths.[1]

TEM images of the CuONP samples synthesized at different copper salt concentrations, presented in Fig. 10, showed a nanoparticle morphology that was concentration-dependent. Indeed, between 0.02 M and 0.1 M, the morphology of CuONPs is quasi-spherical, with a size in the range of 10–13 nm (nanoparticle sizes measured by TEM are mentioned in Fig. 10).

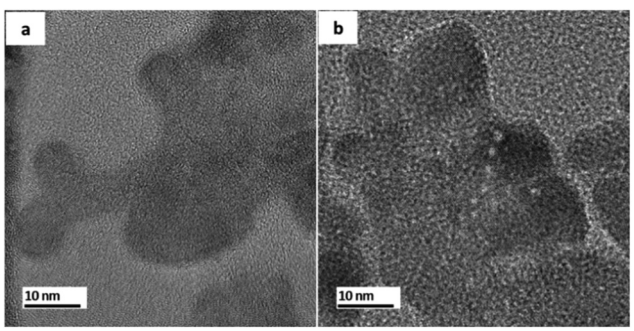

Fig. 8 HRTEM images of CuONPs synthesized at 60 °C and heated at 100 °C.

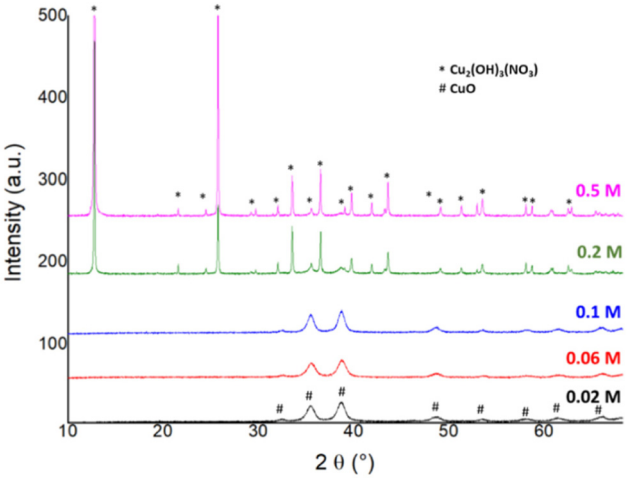

Fig. 9 XRD patterns of the samples synthesized at different copper precursor concentrations (Cu : OH ratio is 1 : 2).

However, at 0.2 M, the morphology of the copper-based nanoparticles became less defined and more agglomerated and the nanoparticle size increased to about 28 nm. The agglomeration of the nanoparticles could be due to the increase of the ionic strength in the medium at this concentration. At a copper concentration of 0.5 M, nanorods were obtained with an average size of 142.8 ± 62.6 nm (14.3 ± 2.3 nm width). These nanorods were formed by an oriented attachment assembly of the nanoparticles, as shown in Fig. S4. The drastic change in the morphology at a high copper concentration suggests a different mechanism of synthesis under these experimental conditions. Indeed, a high concentration of copper favors nucleation in a heterogeneous system.[26] It was reported in the work of Jolivet *et al.* that the protonation/deprotonation rate of the surface oxygen atoms is controlled by the acidity and ionic strength. This process influences the electrostatic surface charge density of the particles, resulting in a change in the surface chemical composition.[42] This change leads to a decrease in the interfacial tension as stated by the Gibbs law:

$$\Delta\gamma = -\sum \Gamma_i \mathrm{d}\mu_i \qquad (4)$$

where $\Delta\gamma$ is the interfacial tension and Γ_i is the adsorption density (mol m^{-2}) of species i under the chemical potential μ_i.[42]

The change of the copper concentration modifies the surface energy of the nanoparticles. This is the driving force for nanoparticle evolution in solution. Indeed, the nanoparticles may undergo transformations depending on the nature of the surrounding solution or any other modification of their environment.[43] In fact, at a high copper concentration, the dihydroxylation and therefore the deprotonation rate decreases, which explains the appearance of a copper hydroxynitrate phase at concentrations of 0.2 and 0.5 M and there will be more adsorbed species on the crystal faces, which could orient the crystal growth and explain the elongated morphology of the obtained copper-based structures. Moreover, the coalescence of the nanoparticles and the oriented attachment (OA) phenomenon are

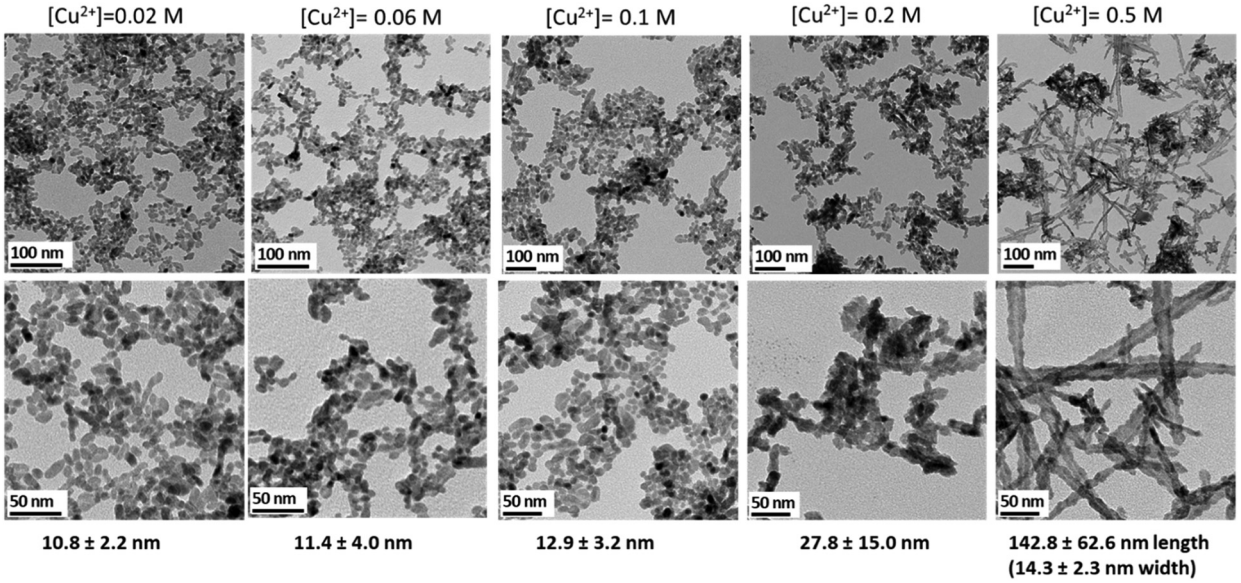

Fig. 10 TEM images of CuONPs synthesized at different copper salt concentrations ([OH^-] = 2x[Cu^{2+}]), indicating the nominal size of the obtained particles.

highlighted for copper concentrations of 0.2 and 0.5 M, which suggests the crystal growth through OA as one of the known mechanisms of nanoparticle growth in the literature.[21] Li *et al.*[44] also discussed this kind of crystal growth for iron oxide nanoparticles. In fact, they explain, using *in situ* HRTEM images and videos, that the nanoparticles aggregate into clusters where they interact in close proximity and then they become nearly aligned through Brownian motion. So, the nanoparticles need attractive forces as the electrostatic interactions to keep them in proximity, explaining why the OA of copper-based nanoparticles in our study occurs at high copper concentrations (0.2 M and 0.5 M). It should be noted that it is well known that the increase in the monomer concentration leads to an increase in the size of the final nanoparticles that normally maintain the same morphology according to the classical crystal growth based on Ostwald ripening.[21] Some authors consider that the OA is the result of different mechanisms that involve adjacent nanoparticles spontaneously aligning with the same crystallographic orientation and then fusing at a shared planar interface.[45] However, for both approaches, the system tends to reduce the total energy by reducing the surface energy. It is the first time that this phenomenon is highlighted and proved for copper oxide growth.

Effect of reaction pH on the morphology of CuONPs

The reaction pH is one of the important experimental parameters that could affect the morphology of nanomaterials.[4,46] In this study, CuONPs were synthesized at three different pH values where only the amount of added NaOH was changed. The chosen Cu^{2+}/OH^- ratios were 1 : 2, 1 : 4 and 1 : 6, leading to pH values of 5.1, 8.4 and 11.6, respectively. The copper concentration is 0.02 M and the reaction temperature is 95 °C. Fig. 11 presents the XRD patterns of the synthesized samples, indicating the presence of only the copper oxide phase in all cases. The crystallite sizes are found to be 11.8 ± 1.3 nm, 12.0 ± 0.9 nm, and 12.4 ± 1.1 nm for the Cu^{2+}/OH^- ratios of 1 : 2, 1 : 4, and 1 : 6, respectively. This result suggests no structural differences between the samples where the low pattern intensity does not reflect significant changes.

Fig. 12 presents the TEM images of the obtained CuONP samples where the results reveal a change in the morphology from quasi-spherical (slightly anisotropic) for Cu^{2+}/OH^- = 1 : 2 (Fig. 12a) with a diameter of 12.7 ± 2.9 nm to nanorods (highly anisotropic) for Cu^{2+}/OH^- = 1 : 4 and 1 : 6. Moreover, the nanorod length tends to increase from 27.2 ± 3.0 nm to 78.4 ±

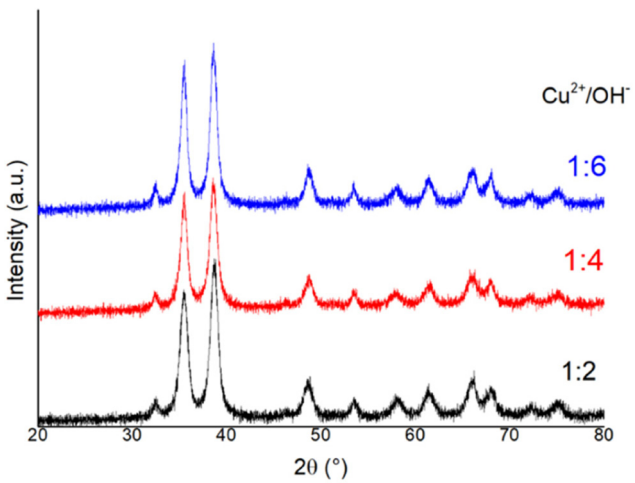

Fig. 11 XRD analyses of CuONPs synthesized at different molar ratios of Cu^{2+}/OH^-: (a) 1 : 2, (b) 1 : 4 and (c) 1 : 6 showing the CuO crystal phase for all samples.

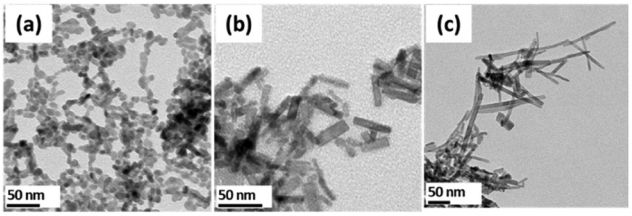

Fig. 12 TEM images of CuONPs synthesized at different molar ratios of OH^-/Cu^{2+}: (a) 2 : 1, (b) 4 : 1 and (c) 6 : 1.

42.1 nm when the Cu^{2+}/OH^- ratio increases from 1 : 4 to 1 : 6, respectively.

It should be noted that the CuONP surface exhibits more or less basic properties, depending on the equilibrium and protonation constants in solution and depending on the solution pH. The protonation–deprotonation equilibria of surface oxygen sites affect the electrostatic charge on particle surfaces, influencing their crystal face energies. Indeed, the acidity governs the protonation/deprotonation rate of the surface oxygen surface according to the following formula:

$$Cu\text{–}O^- + H^+ \leftrightarrow Cu\text{–}OH$$

$$Cu\text{–}OH + H^+ \leftrightarrow Cu\text{–}OH_2{}^+$$

The change in the surface charge leads to changes in the interfacial tension as stated by the Gibbs law in the formula.[4] For anisotropic particles, each crystal face's energy must be considered to determine the particle morphology.[43] This could explain the elongated (rod-shaped) morphology of CuONPs at higher pH. In fact, for anisotropic nanoparticles, all the crystal faces do not have the same surface energy in solution, which orients the crystal growth to the preferential direction, leading to different shapes. The study of Zhu *et al.*[19] suggests that copper could be coordinated to 6 OH^- in the form of an octahedron $[Cu(OH)_6]^{4-}$ where the binding energies of OH^- at the axis are lower than those at the plane, making them more easily replaced and dehydrated to form CuO crystallites. This leads to higher growth rates along the axis compared to the plane, causing anisotropic CuO nanocrystal formation. Additionally, the excess of OH^- induces repulsive electrostatic interactions between the nanoparticles, which reduces their agglomeration.

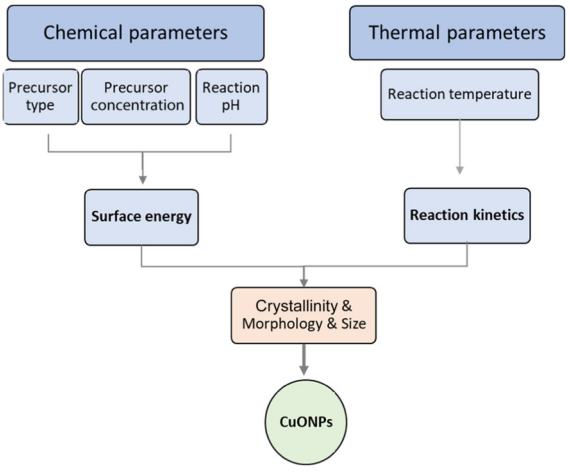

Fig. 13 Diagram summarizing the studied parameters and their effect on the morphology and size of CuONPs.

Conclusions

This study provides a comprehensive investigation into the controlled synthesis of copper oxide nanoparticles (CuONPs) using a precipitation method without surfactants. By systematically varying key experimental parameters, including precursor type and concentration, and reaction temperature and pH, this work demonstrates how each factor significantly influences the size, morphology, and crystallinity of the resulting nanoparticles (Fig. 13). The findings highlight the critical role of the precursor's counter-ion in directing the crystal growth and the morphology where only the copper nitrate and sodium hydroxide couple gives quasi-spherical-shaped particles among the studied samples. The counter ions could change the surface energy of crystal faces, promoting the synthesis of anisotropic shapes. The same effect was highlighted for the increased Cu/OH ratio where the change of the reaction pH changes the electrostatic charge on the particle surfaces and consequently their crystal face energies. Similarly, the increase in copper concentration changes the interfacial tension and leads to an oriented attachment growth mechanism of the nanoparticles, forming rod-like shapes. However, the temperature of the reaction increases the kinetics of CuONP synthesis. In fact, a metastable copper hydroxide phase was obtained at low temperature (up to 50 °C) and a thermodynamically stable copper oxide phase was obtained at higher temperature. Interestingly, this work indicates an intermediate flake-like structure that transformed into nano-size spherical particles with increasing temperature. Additionally, the proposed growth mechanism contributes to a deeper understanding of CuONP synthesis, illustrating for the first time the direct observation of structural rearrangement under the reaction temperature effect. Two possible mechanisms were discussed, one at low temperature where the CuO condensation mechanism is slow, leading to flake-shaped particles, and one at high reaction temperature where the oxolation reaction competes with the olation one, leading to a quasi-spherical shape. Finally, this work proposes a comprehensive framework for controlling the morphology of CuONPs without the use of surfactants under mild reaction conditions, paving the way for reproducible fabrication strategies tailored for specific applications. Indeed, the shape and size of CuO nanoparticles can strongly influence their specific surface area and colloidal stability. An increase in the specific surface area enhances the sensitivity of CuO-based sensors and the catalytic activity of CuO nanoparticles, and also affects their antimicrobial pro-

perties. In addition, the luminescence properties of CuO-based materials are strongly dependent on the particle shape.

Author contributions

Fadoua Sallem: conceptualization, investigation and writing – original draft. Corinne Chaneac: review, editing and validation. Mickael Wagner: data curation and investigation. Nicolas Rataj: investigation. Eloise Annabi: investigation. Alain Castillo: resources. Ludovic Menjot: resources. Astrid Avellan: review, validation, supervision, project administration and funding acquisition.

Conflicts of interest

There are no conflicts to declare.

Data availability

The data supporting this article have been included as part of the supplementary information (SI). Supplementary information is available. See DOI: https://doi.org/10.1039/d5nr04826e.

Acknowledgements

The authors would like to thank the Castaing Centre for transmission electron microscopy facilities and Laurent Weingarten for HRTEM images. This work received funding from the European Research Council (ERC) under the European Union's Horizon 2020 research and innovation program (ERC StG, LEAPHY 101041729).

References

1 T. H. Tran and V. T. Nguyen, Copper Oxide Nanomaterials Prepared by Solution Methods, Some Properties, and Potential Applications: A Brief Review, *Int. Scholarly Res. Not.*, 2014, **2014**(1), 856592.
2 Payal and P. Pandey, Role of Nanotechnology in Electronics: A Review of Recent Developments and Patents, *Recent Pat. Nanotechnol.*, 2022, **16**(1), 45–66.
3 N. Verma and N. Kumar, Synthesis and Biomedical Applications of Copper Oxide Nanoparticles: An Expanding Horizon, *ACS Biomater. Sci. Eng.*, 2019, **5**(3), 1170–1188.
4 T. Ringu, A. Das, S. Ghosh and N. Pramanik, Exploring the potential of copper oxide nanoparticles (CuO NPs) for sustainable environmental bioengineering applications, *Nanotechnol. Environ. Eng.*, 2024, **9**(4), 679–707.
5 J. O. Ighalo, P. A. Sagboye, G. Umenweke, O. J. Ajala, F. O. Omoarukhe, C. A. Adeyanju, *et al.*, CuO nanoparticles (CuO NPs) for water treatment: A review of recent advances, *Environ. Nanotechnol., Monit. Manage.*, 2021, **15**, 100443.
6 C. I. Idumah, Influence of nanotechnology in polymeric textiles, applications, and fight against COVID-19, *J. Text. Inst.*, 2021, **112**(12), 2056–2076.
7 L. H. Nguyen, V. S. Le, L. D. Tran, N. V. Thai, H. T. N. Tram, B. Q. Minh, *et al.*, Environmental-friendly method for preparing CoFe2O4 coated biopolymer extracted from dragon fruit peel: Characterization and application as nanocomposite adsorbent for removal of As(III) pollutants from aqueous solution, *J. Ind. Eng. Chem.*, 2023, **118**, 432–445.
8 V. Rajput, T. Minkina, S. Sushkova, A. Behal, A. Maksimov, E. Blicharska, *et al.*, ZnO and CuO nanoparticles: a threat to soil organisms, plants, and human health, *Environ. Geochem. Health*, 2020, **42**(1), 147–158.
9 N. Kumari, S. Rani and V. Sharma, Green Agriculture: Nanoparticles as Tools to Mitigate Heavy Metal Toxicity, *Rev. Environ. Contam. Toxicol.*, 2023, **262**(1), 1.
10 X. D. Yang, L. L. Jiang, C. J. Mao, H. L. Niu, J. M. Song and S. Y. Zhang, Sonochemical synthesis and nonlinear optical property of CuO hierarchical superstructures, *Mater. Lett.*, 2014, **115**, 121–124.
11 H. Liu, S. Wang, R. Zhuo, Y. Duan, J. Wang, Y. Li, *et al.*, Size-controlled synthesis of copper oxide nanoparticles with a supercritical hydrothermal synthesis method, *Powder Technol.*, 2024, **444**, 119803.
12 V. Pradeep, P. Veerakumar and V. P. Veeraraghavan, Facile Microwave-Assisted Hydrothermal Synthesis of Copper Oxide Nanoneedle Arrays for Practical Biomedical Applications, *Cureus*, 2024, **16**(1), e51678.
13 T. T. Tran, A. H. Huynh Vo, T. T. Nguyen, A. D. Nguyen, M. H. Huynh Tran, V. C. Tran, *et al.*, pH-Dependent Morphology of Copper(II) Oxide in Hydrothermal Process and Their Photoelectrochemical Application for Non-Enzymatic Glucose Biosensor, *Appl. Sci.*, 2024, **14**(13), 5688.
14 S. Zahra, T. Abbas, A. Sheikh, H. Bukhari and S. Zahra, Synthesis and characterization of nanosize copper oxide by non-aqueous sol–gel process, *J. Iran. Chem. Soc.*, 2024, **21**(8), 2211–2220.
15 Q. Zhang, K. Zhang, D. Xu, G. Yang, H. Huang, F. Nie, *et al.*, CuO nanostructures: Synthesis, characterization, growth mechanisms, fundamental properties, and applications, *Prog. Mater. Sci.*, 2014, **60**, 208–337.
16 M. Vaseem, A. Umar, S. H. Kim and Y. B. Hahn, Low-Temperature Synthesis of Flower-Shaped CuO Nanostructures by Solution Process: Formation Mechanism and Structural Properties, *J. Phys. Chem. C*, 2008, **112**(15), 5729–5735.
17 Y. Liu, L. Liao, J. Li and C. Pan, From Copper Nanocrystalline to CuO Nanoneedle Array: Synthesis, Growth Mechanism, and Properties, *J. Phys. Chem. C*, 2007, **111**(13), 5050–5056.
18 H. Siddiqui, M. S. Qureshi and F. Z. Haque, Effect of copper precursor salts: Facile and sustainable synthesis of controlled shaped copper oxide nanoparticles, *Optik*, 2016, **127**(11), 4726–4730.

19 J. Zhu, H. Bi, Y. Wang, X. Wang, X. Yang and L. Lu, CuO nanocrystals with controllable shapes grown from solution without any surfactants, *Mater. Chem. Phys.*, 2008, **109**(1), 34–38.
20 D. P. Singh, A. K. Ojha and O. N. Srivastava, Synthesis of Different $Cu(OH)_2$ and CuO (Nanowires, Rectangles, Seed-, Belt-, and Sheetlike) Nanostructures by Simple Wet Chemical Route, *J. Phys. Chem. C*, 2009, **113**(9), 3409–3418.
21 N. T. K. Thanh, N. Maclean and S. Mahiddine, Mechanisms of Nucleation and Growth of Nanoparticles in Solution, *Chem. Rev.*, 2014, **114**(15), 7610–7630.
22 M. Shahmiri, N. A. Ibrahim, N. Zainuddin, B. Bakhtyar, A. Zaharim and K. Sopian, Effect of pH on the Synthesis of CuO Nanosheets by Quick Precipitation Method, *WSEAS Transactions on Environment and Development*, 2013, **9**(2), 137–146.
23 E. Bruno, M. Haris, A. Mohan and M. Senthilkumar, Temperature effect on CuO nanoparticles via facile hydrothermal approach to effective utilization of UV–visible region for photocatalytic activity, *Appl. Phys. A*, 2021, **127**(12), 925.
24 Z. N. Kayani, M. Umer, S. Riaz and S. Naseem, Characterization of Copper Oxide Nanoparticles Fabricated by the Sol–Gel Method, *J. Electron. Mater.*, 2015, **44**(10), 3704–3709.
25 M. Saadat, O. Amiri and M. GoshtasbiRad, Synthesis of Nano-CuO Powder via Sol– Gel and Investigation the Effective Factors on the Final Size, *J. Nanostruct.*, 2024, **14**(3), 800–808.
26 H. Siddiqui, M. R. Parra and F. Z. Haque, Optimization of process parameters and its effect on structure and morphology of CuO nanoparticle synthesized via the sol–gel technique, *J. Sol-Gel Sci. Technol.*, 2018, **87**(1), 125–135.
27 B. L. Cushing, V. L. Kolesnichenko and C. J. O'Connor, Recent Advances in the Liquid-Phase Syntheses of Inorganic Nanoparticles, *Chem. Rev.*, 2004, **104**(9), 3893–3946.
28 S. Shankar and J. W. Rhim, Effect of Zn salts and hydrolyzing agents on the morphology and antibacterial activity of zinc oxide nanoparticles, *Environ. Chem. Lett.*, 2019, **17**(2), 1105–1109.
29 L. K. Plummer and J. E. Hutchison, Understanding the Effects of Iron Precursor Ligation and Oxidation State Leads to Improved Synthetic Control for Spinel Iron Oxide Nanocrystals, *Inorg. Chem.*, 2020, **59**(20), 15074–15087.
30 F. N. Sayed and V. Polshettiwar, Facile and Sustainable Synthesis of Shaped Iron Oxide Nanoparticles: Effect of Iron Precursor Salts on the Shapes of Iron Oxides, *Sci. Rep.*, 2015, **5**(1), 9733.
31 H. Siddiqui, M. S. Qureshi and F. Z. Haque, Surfactant assisted wet chemical synthesis of copper oxide (CuO) nanostructures and their spectroscopic analysis, *Optik*, 2016, **127**(5), 2740–2747.
32 J. P. Jolivet, S. Cassaignon, C. Chanéac, D. Chiche, O. Durupthy and D. Portehault, Design of metal oxide nanoparticles: Control of size, shape, crystalline structure and functionalization by aqueous chemistry, *C. R. Chim.*, 2010, **13**(1), 40–51.
33 R. Srivastava, M. U. Anu Prathap and R. Kore, Morphologically controlled synthesis of copper oxides and their catalytic applications in the synthesis of propargylamine and oxidative degradation of methylene blue, *Colloids Surf., A*, 2011, **392**(1), 271–282.
34 W. M. Rangel, R. A. A. Boca Santa and H. G. Riella, A facile method for synthesis of nanostructured copper(II) oxide by coprecipitation, *J. Mater. Res. Technol.*, 2020, **9**(1), 994–1004.
35 T. N. Ramesh and T. L. Madhu, Thermal Decomposition Studies of Layered Metal Hydroxynitrates (Metal: Cu, Zn, Cu/Co, and Zn/Co), *Int. J. Inorg. Chem.*, 2015, **2015**(1), 536470.
36 B. Liu and H. C. Zeng, Mesoscale Organization of CuO Nanoribbons: Formation of "Dandelions", *J. Am. Chem. Soc.*, 2004, **126**(26), 8124–8125.
37 H. M. Xiao, S. Y. Fu, L. P. Zhu, Y. Q. Li and G. Yang, Controlled Synthesis and Characterization of CuO Nanostructures through a Facile Hydrothermal Route in the Presence of Sodium Citrate, *Eur. J. Inorg. Chem.*, 2007, **2007**(14), 1966–1971.
38 O. Akhavan and E. Ghaderi, Copper oxide nanoflakes as highly sensitive and fast response self-sterilizing biosensors, *J. Mater. Chem.*, 2011, **21**(34), 12935–12940.
39 A. Labanni, M. Nasir and S. Arief, Research progress and prospect of copper oxide nanoparticles with controllable nanostructure, morphology, and function via green synthesis, *Mater. Today Sustain.*, 2023, **24**, 100526.
40 J. P. Jolivet, C. Chanéac and E. Tronc, Iron oxide chemistry. From molecular clusters to extended solid networks, *Chem. Commun.*, 2004, (5), 481–483.
41 M. Xu, F. Wang, B. Ding, X. Song and J. Fang, Electrochemical synthesis of leaf-like CuO mesocrystals and their lithium storage properties, *RSC Adv.*, 2012, **2**(6), 2240–2243.
42 J. P. Jolivet, C. Froidefond, A. Pottier, C. Chanéac, S. Cassaignon, E. Tronc, *et al.*, Size tailoring of oxide nanoparticles by precipitation in aqueous medium. A semi-quantitative modelling, *J. Mater. Chem.*, 2004, **14**(21), 3281–3288.
43 M. Auffan, J. Rose, C. Chanéac, J. P. Jolivet, A. Masion and M. R. Wiesner, *et al.*, *Surface Reactivity of Manufactured Nanoparticles*, in *Nanoethics and Nanotoxicology*, ed. P. Houdy, M. Lahmani and F. Marano, Springer, Berlin, Heidelberg, 2011, pp. 269–290.
44 D. Li, M. H. Nielsen, J. R. I. Lee, C. Frandsen, J. F. Banfield and J. J. De Yoreo, Direction-Specific Interactions Control Crystal Growth by Oriented Attachment, *Science*, 2012, **336**(6084), 1014–1018.
45 M. Niederberger and H. Cölfen, Oriented attachment and mesocrystals: Non-classical crystallization mechanisms based on nanoparticle assembly, *Phys. Chem. Chem. Phys.*, 2006, **8**(28), 3271–3287.
46 J. Liu, J. Jin, Z. Deng, S. Z. Huang, Z. Y. Hu, L. Wang, *et al.*, Tailoring CuO nanostructures for enhanced photocatalytic property, *J. Colloid Interface Sci.*, 2012, **384**(1), 1–9.